Heliyon

ELSEVIER

Received:
25 November 2016
Revised:
20 January 2017
Accepted:
17 March 2017

Heliyon 3 (2017) e00273

Synthesis of nickel and cobalt sulfide nanoparticles using a low cost sonochemical method

Matjaž Kristl [a,*], Brina Dojer [b], Sašo Gyergyek [a,c], Janja Kristl [d]

[a] *Faculty of Chemistry and Chemical Engineering, University of Maribor, Smetanova 17, SI – 2000, Maribor, Slovenia*

[b] *Faculty of Natural Sciences and Mathematics, University of Maribor, Koroška cesta 160, SI – 2000, Maribor, Slovenia*

[c] *Jožef Stefan Institute, Department for Materials Synthesis, Jamova cesta 39, SI – 1000, Ljubljana, Slovenia*

[d] *Faculty of Agriculture and Life Sciences, University of Maribor, Pivola 10, SI – 2311, Hoče, Slovenia*

* Corresponding author.

E-mail address: matjaz.kristl@um.si (M. Kristl).

Abstract

Nickel and cobalt sulfides are promising materials in different cutting-edge research areas like solar cells, supercapacitors, catalysts, and electrode materials. Nickel and cobalt sulfides with various stoichiometries have been synthesized sonochemically from $Ni(CH_3COO)_2 \cdot 4H_2O$, $Co(CH_3COO)_2 \cdot 2H_2O$ and different sulfur precursors using a direct immersion ultrasonic probe. The products were characterized by X-ray powder diffraction, transmission electron microscopy (TEM) including EDX analysis, IR and UV–Vis spectroscopy and elemental analysis. Following products have been obtained: NiS, Ni_3S_4, $CoS_{1.097}$ and Co_9S_8, with average crystallite sizes in the range 7−30 nm. Effects of different reaction conditions on the size, morphology and optical band-gap energy were evaluated. Optical band-gap energies in the range 3.3 eV−3.8 eV were observed for the obtained nanoparticles.

Keywords: Materials science, Inorganic chemistry, Nanotechnology

1. Introduction

Transition metal chalcogenides have attracted considerable attention during the past decade due to their unique physical and chemical properties, including their

http://dx.doi.org/10.1016/j.heliyon.2017.e00273

use as semiconducting, optical, magnetic, and catalytic materials [1, 2]. Important transition metal sulfides include, among others, cadmium sulfide [3, 4, 5], zinc sulfide [6], silver sulfide [7, 8] as well as many different phases of copper sulfides [7, 9, 10, 11].

Among those materials, nickel sulfides have been widely studied due to their various phases and stoichiometries, ranging from the nickel-rich compound Ni_3S_2, Ni_6S_5, Ni_7S_6, Ni_9S_8, NiS to sulfur-rich compounds like Ni_3S_4 and NiS_2 [12, 13]. NiS is known to exist in two main phases, i.e. the hexagonal α-NiS, stable at elevated temperatures, and the rhomboedral β-NiS, which is stable at low temperatures [14]. NiS has been recently used in many applications, such as materials for highly effective counter electrodes for solar cells [15, 16, 17] and seems to be an ideal material for supercapacitors [18, 19, 20] and cathodes for lithium batteries [21, 22, 23]. It has been reported that cathode materials are currently the limiting factor preventing a wider application of lithium batteries in electric and hybrid vehicles and some of these shortages could be overcome by using metal sulfides as active cathode materials, and amongst them, NiS with a high theoretical capacity seems to be the most promising [12].

Many methods were reported for the preparation of NiS, the most straightforward being the high temperature synthesis from elements or the reaction of sulfide ions to an aqueous solution of nickel(II) ions [24]. Many other techniques to prepare nickel sulfides were reported later, including mechanochemical preparation [25], hydro/solvothermal methods [26, 27, 28], spray pyrolysis [12], decomposition of single-source precursors [13, 29], polyol synthesis [14], microwave synthesis [30] and preparation by the solventless route in air [31].

Very much like nickel sulfides, cobalt sulfides also exist in several stoichiometric and non-stoichiometric phases, such as Co_4S_3, Co_9S_8, CoS, $Co_{1-x}S$, Co_3S_4, Co_2S_3, and CoS_2 [32, 33]. When compared to other semiconducting transition metal sulfides, only a little work has been done on cobalt sulfides until very recently. The phase diagram of the Co-S system is complicated due to the coexistence of strongly reducible cobalt and oxidizable sulfur ion [34]. Cobalt sulfides are reported to have potential applications as catalysts [35, 36], capable of splitting water to produce hydrogen [37], magnetic materials [34, 38], counter electrodes for solar cells [39, 40, 41], anode materials for advanced lithium ion batteries [42, 43, 44] and high-performance supercapacitors [45, 46, 47, 48].

Traditionally, cobalt sulfides were prepared by solid state methods or by reactions of cobalt and hydrogen sulfide [49]. More recently, Hoodles et al. [35] prepared Co_9S_8 by heating Co_3O_4 in a stream of 9.8% H_2S in H_2. Milder routes for the synthesis of nanosized cobalt sulfides have been developed during the last decade, like decomposition of cobalt−thiourea complexes [33, 50], wet chemical methods [36, 41, 42], microwave assisted methods [32, 48], and in the first place the

http://dx.doi.org/10.1016/j.heliyon.2017.e00273

hydrothermal/solvothermal method [34, 39, 43, 46, 47, 49, 50, 51, 52]. It should be mentioned that You et al. report significant advantages of CoS prepared by a microwave synthesis when compared to counterparts prepared by the solvothermal method [48].

Following the pioneering work by Suslick and colleagues, who reported the first sonochemical approach to a metal chalcogenide synthesis by irradiating a slurry of $Mo(CO)_6$ and elemental S in isodurene obtaining nanostructured MoS_2 [53], ultrasound has become an important tool in the synthesis of nanosized metals, metal oxides, ferrite nanoparticles and metal chalcogenides. The unique reaction conditions during the process of acoustic cavitation provide a unique interaction between energy and matter, with 'hot-spots' inside the collapsing bubbles reaching temperatures up to 5000 K and pressures in the range of 1000 bar, following by rapid cooling rates of $>10^{10}$ K/s [54]. This extraordinary reaction conditions enable the synthesis of nanostructured materials with uniform shapes and narrow size distribution. The sonochemical method has been successfully applied to the preparation of numerous nanostructured metal chalcogenides [55, 56], including copper chalcogenides reported recently by our group [11, 57].

The first sonochemical preparation of NiS nanoparticles was reported in 2002 by Wang et al. [58] by irradiating an aqueous solution of nickel acetate, thioacetamide (TAA) and triethanolamine as complexing agent under ambient air. More recently, De la Parra-Arciniega et al. [59] reported a novel synthesis methodology for preparation of NiS submicron particles by ultrasonic irradiation of a solution containing nickel nitrate and TAA in different mixtures of ethanol/ionic liquid. To the best of our knowledge, no sonochemical synthesis of cobalt sulfides has been reported up to now, although nanocrystals of some other cobalt binary compounds, e.g. Co_3O_4 [60], have been successfully prepared using the sonochemical method. The present study aimed at successful synthesis of nickel and cobalt sulfides nanoparticles using low cost sonochemical method. For this, aqueous precursor solutions of different stoichiometric molar ratios of Ni, Co and sulfides were prepared from their corresponding acetates.

2. Experimental

All the chemicals used during the synthesis were used as purchased without further purification. Both nickel and copper precursors, $Ni(CH_3COO)_2 \cdot 4H_2O$ ($\geq$ 99.0%), $Co(CH_3COO)_2 \cdot 2H_2O$ ($\geq$ 99.0%), were obtained from Sigma-Aldrich. Following sulfur precursors were used: thioacetamide, C_2H_5NS (99%, Sigma-Aldrich), thiourea, CH_4N_2S (99.8%, Merck), and sodium thiosulfate pentahydrate, $Na_2S_2O_3 \cdot 5H_2O$ (99.5%, Alkaloid). EDTA (99.8%, Kemika Zagreb), and TEA (triethanolamine, 99%, Carlo Erba) were used as complexing agents.

http://dx.doi.org/10.1016/j.heliyon.2017.e00273

In a typical synthesis of nickel sulfides, we dissolved 2.49 g (= 0.01 mol) of Ni $(CH_3COO)_2 \cdot 4H_2O$ and 0.75 g (= 0.01 mol) of C_2H_5NS in 50 mL of water in a 100 mL flat-bottomed beaker. The mixture was sonicated in an ambient atmosphere for 1 h using a Sonics and Materials VCX 600 sonicator (20 kHz, 1 cm^2 Ti direct immersion horn) at different amplitudes, namely 30%, 50%, 70% and 90%. The starting deep green solution turned black after some minutes of sonication, depending on the used amplitude. The black precipitate obtained after 1 h of sonication was centrifuged at 7000 RPM, washed twice with water and twice with absolute ethanol and air-dried for 24 h. The supernatant was intense green at amplitudes of 30% and 50%, indicating incomplete reaction, while it was slightly green at 70 and 90% amplitude. All further syntheses were performed at 70% amplitude. In additional experiments, we changed the molar ratio of precursors from n(Ni): n(S) = 1: 1 to n(Ni): n(S) = 1: 2 and 1: 3, and prolonged the reaction time to 2 h, using the same experimental procedure as described above. Further syntheses were carried out using aqueous solutions of complexing agents EDTA and 3-ethanolamine (TEA) and by replacing thioacetamide as sulfur precursor by thiourea and sodium thiosulfate.

The same general procedure was used for the sonochemical preparation of cobalt sulfides: we dissolved 2.13 g (= 0.01 mol) of $Co(CH_3COO)_2 \cdot 2H_2O$ and 0.75 g (= 0.01 mol) of C_2H_5NS in 50 mL of water and sonicated the solution for 1 h at 70% amplitude. The red solution turned black after 5 min reaction time. The black precipitate obtained after 1 h of sonication was handled as described above. Further experiments involved changing the molar ratio of precursors in the range of n(Co): n(S) = 1.2: 1 to n(Co): n(S) = 1: 2 and using thiourea and sodium thiosulfate. We heated the as-obtained amorphous products using a Mettler TGA/SDTA 851^e system and Al_2O_3 crucibles in the temperature range 30–500 °C in a nitrogen stream of 100 mL/min with a heating rate of 10 K/min. Further details about experimental conditions during the syntheses of nickel and cobalt sulfides can be obtained in Table 1.

X-ray powder diffraction spectra were measured using an AXS-Bruker/Siemens model D5005 X-ray powder diffractometer (XRD) equipped with a CuKα radiation source and a graphite monochromator (λ = 1.54178 Å) in the range $20° \leq 2\theta \leq 80°$, using a step size of 0.014° and time/step = 1s. The crystallite size of the nanoparticles, d_{hkl}, was estimated using the Scherrer formula:

$$d_{hkl} = \frac{0.94\lambda}{\beta_{hkl} \cos\theta_{hkl}}$$

Here, λ is the wavelength of the X-ray radiation (nm), β_{hkl} the full-width at half-maximum (FWHM) of the corresponding peak (°) and θ_{hkl} is the Bragg diffraction angle (°). The effects of instrumental broadening were subtracted by measuring an external macrocrystalline standard under the same instrumental conditions.

http://dx.doi.org/10.1016/j.heliyon.2017.e00273

http://dx.doi.org/10.1016/j.heliyon.2017.e00273

Table 1. Precursors, molar ratios, reaction conditions and products of the sonochemical syntheses of nickel and cobalt sulfides. $Ni(CH_3COO)_2 \cdot 4H_2O$ and $Co(CH_3COO)_2 \cdot 2H_2O$ were used as Ni and Co precursors during all syntheses, respectively. Reaction yields were calculated only in cases where nickel or cobalt chalcogenides without detectable impurities were obtained.

Sample	Sulfur precursor	Ni: S molar ratio	Complexing agent	Sonication time (min)	Amplitude (%)	Product(s)	Crystallite size (nm)	Reaction yield (%)
Ni1	C_2H_5NS	1:1	-	60	30	-	-	-
Ni2	C_2H_5NS	1:1	-	60	50	NiS	13	25.3
Ni3	C_2H_5NS	1:1	-	60	70	NiS	17	45.5
Ni3-1	C_2H_5NS	1:1	-	30	70	NiS	17	28.9
Ni3-2	C_2H_5NS	1:1	-	120	70	NiS	19	46.4
Ni4	C_2H_5NS	1:1	-	60	90	NiS	18	41.2
Ni5	C_2H_5NS	1:2	-	60	70	NiS	14	46.9
Ni6	C_2H_5NS	1:3	-	60	70	NiS	16	71.6
Ni7	C_2H_5NS	1:1	EDTA, 0.05M	60	70	-	-	-
Ni8	C_2H_5NS	1:1	TEA, ≈10%	60	70	NiS	18	75.3
Ni9	CH_4N_2S	1:1	-	120	70	$Ni(OH)_2$	-	-
Ni10	$Na_2S_2O_3 \cdot 5H_2O$	1:1	-	60	70	NiS, Ni_3S_4	24 (NiS)	5.0 (NiS)
Ni11	$Na_2S_2O_3 \cdot 5H_2O$	1:2	-	60	70	Ni_3S_4, (NiS)	7 (Ni_3S_4)	10.3 (Ni_3S_4)
		Co: S molar ratio						
Co1	C_2H_5NS	1:1	-	60	70	$CoS_{1.097}$	26	32.1
Co2	C_2H_5NS	1.2:1	-	60	70	Co_9S_8	30	49.6
Co3	C_2H_5NS	1:2	-	60	70	$CoS_{1.097}$	22	33.3
Co5	CH_4N_2S	1:1	-	60	70	CoO	-	-
Co6	$Na_2S_2O_3 \cdot 5H_2O$	1:1	-	60	70	CoO	-	-

A Varian SpectrAA-10 flame atomic spectrometer equipped with a deuterium background corrector was used for the determination of Ni and Co within the samples. All solutions were prepared using high-purity water. Nickel and cobalt calibration standard solutions were prepared by diluting the standard stock solutions containing 1000 mg/L (Certipur, Merck). The samples were placed in PTFE vessels and heated in microwave oven CEM (MDS 2000) with concentrated HNO_3. After digestion, the solutions were cooled to room temperature and diluted to a total volume of 50 mL.

For the TEM investigation, the nanoparticles were dispersed in ethanol using an ultrasonic bath, deposited on a copper-grid-supported perforated transparent carbon foil and recorded on a JEOL 2100 TEM operating at 200 kV. UV–Vis absorption spectra of samples dispersed in ethanol by sonication in an ultrasonic bath were recorded on a Varian Cary 50 Bio UV–Vis spectrophotometer. Infrared spectra were taken on a SHIMADZU IRAffinity-1 FTIR spectrometer using ATR in the range 380−4000 cm^{-1}.

3. Results and discussion

3.1. Nickel sulfides

Powder XRD patterns of products, obtained by the sonochemical synthesis from Ni $(CH_3COO)_2 \cdot 4H_2O$ and C_2H_5NS (molar ratio 1:1, 1 h sonication time) using different sonicator amplitudes, are shown in Fig. 1. The average crystallite size was calculated from the average of the (100) and (110) peaks. It can clearly be seen that

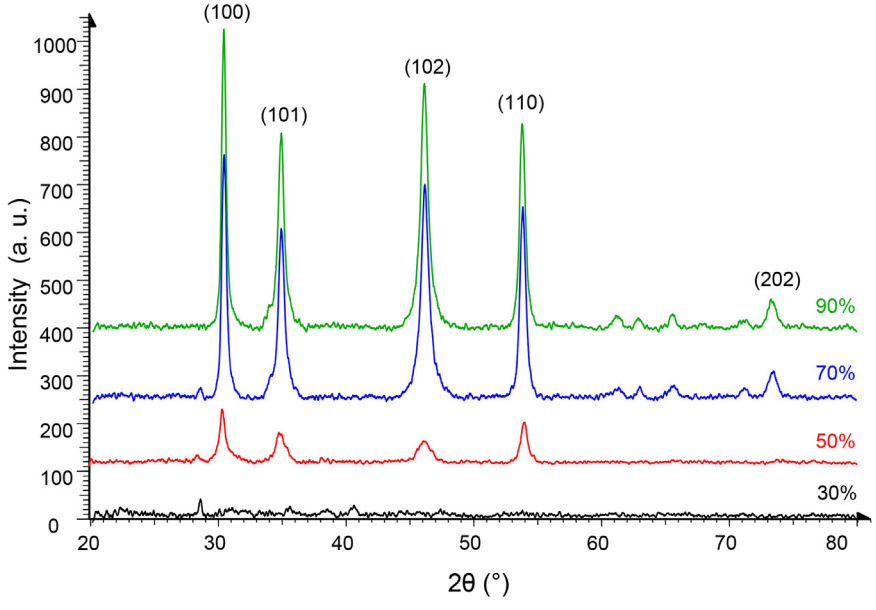

Fig. 1. X-ray powder diffraction patterns of nickel sulfide synthesized from $Ni(CH_3COO)_2 \cdot 4H_2O$ and C_2H_5NS (molar ratio 1:1, 1 h sonication time) by using different sonicator amplitudes.

http://dx.doi.org/10.1016/j.heliyon.2017.e00273

the synthesis performed at 30% amplitude yielded no observable crystalline products, while hexagonal α-nickel sulfide (PDF No. 00-002-1280) nanoparticles were obtained by using higher amplitudes. The crystallite size of the as-prepared NiS increased from 13 nm at 50% amplitude to 18 nm at 90% amplitude while the highest reaction yield was obtained at 70% amplitude. Following the results of these syntheses, 70% amplitude was used during all subsequent experiments, since using 90% amplitude did not increase the reaction yield. Shortening the reaction time to 30 min (Ni3-1, pattern not shown) caused the reaction yield to decrease significantly, while the shape of the diffraction pattern and the crystallite size remained virtually unchanged. On the other hand, the diffraction pattern as well as the reaction yield of NiS obtained by using a longer reaction time of 120 min (Ni3-2, pattern not shown) was not significantly different when compared to the product obtained after 60 min. Following the results of those experiments, all the following syntheses were carried out by using 60 min sonication time. Further details about reaction products can be obtained from Table 1 (samples Ni1− Ni4).

It should be pointed out that during all syntheses performed in molar ratio 1:1, the supernatants after the reactions remained green, indicating the incomplete reaction of nickel. We attempted to ensure the complete reaction of nickel ions by carrying out additional syntheses using excess amounts of sulfur, n(Ni): n(S) = 1:2 and 1:3. The XRD patterns (Fig. 2) reveal that nanosized NiS was observed in all cases while the reaction yield, calculated from the amount of Ni, increased significantly when using the 1:3 reaction ratio.

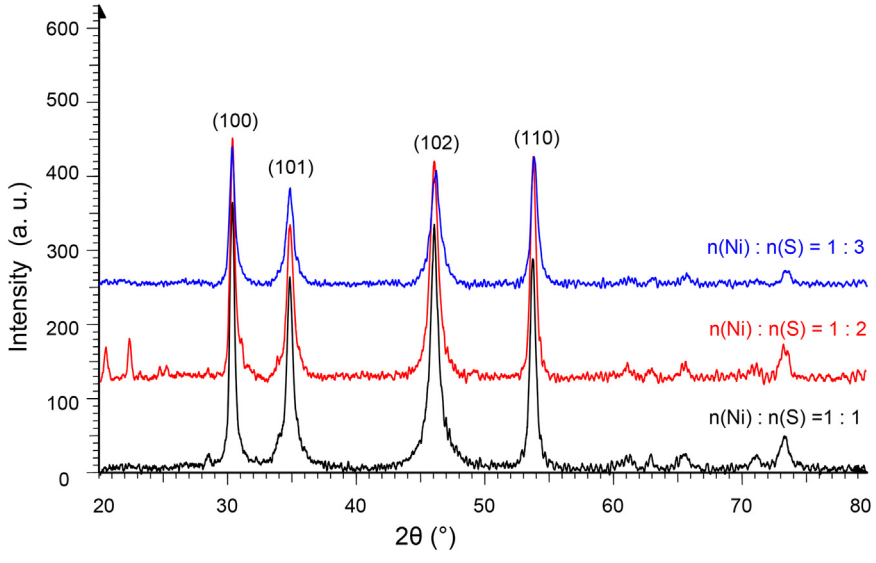

Fig. 2. X-ray powder diffraction patterns of nickel sulfide synthesized from $Ni(CH_3COO)_2 \cdot 4H_2O$ and C_2H_5NS by using different molar ratio of precursors.

http://dx.doi.org/10.1016/j.heliyon.2017.e00273

It is well-known from literature, including previous reports published by our group [11, 57], that complexing agents may play a crucial role during the preparation of nanosized chalcogenides, so additional syntheses were performed in presence of EDTA and TEA. Surprisingly, the black precipitate obtained in low yield in presence of EDTA (sample 7) showed no detectable peaks on the XRD pattern, while the synthesis in presence of TEA (sample 8) was very successful, obtaining pure NiS in substantially higher yield (75.3%) when compared to the synthesis performed under the same conditions without any complexing agent (45.5%).

Previous reports have suggested that ultrasonic decomposition of thioacetamide and subsequent formation of metal sulfides can be summarized as follows [58]:

$H_2O))) \rightarrow H\cdot + OH\cdot$

$C_2H_5NS + 2H\cdot \rightarrow H_2S + C_2H_5N\cdot$

$M^{2+} + H_2S \rightarrow MS + 2H^+$ (M = Ni, Co)

$n\mathrm{MS} \rightarrow (\mathrm{MS})n$

The first reaction represents the formation of primary radicals by sonolysis of water. The *in situ* generated H· radical is highly reducing and readily reacts with TAA to form H_2S, which subsequently reacts with M^{2+} ions to form MS nuclei. The role of the complexing agent TEA during the reaction may be explained through the formation of a M-TEA complex before the beginning of the sonication, which then slowly releases M^{2+} ions during the reaction.

The morphology of NiS nanoparticles prepared by the sonochemical method using various amplitudes is shown in Fig. 3 (a–d). All products are strongly agglomerated. The product obtained by 50% amplitude consists of nearly spherical particles with diameters in the range 10–20 nm (Fig. 3a) as well as nanorod-shaped particles with diameter in the range of 10 nm and lengths between 40 and 100 nm (Fig. 3b). Products prepared by using higher amplitudes (Fig. 3c, d) are more spherical in shape with diameters between 15 and 20 nm, also strongly agglomerated into clusters. The EDX analysis of the samples showed the atomic ratio Ni:S = 1:1, thus confirming the results obtained by powder XRD analysis. Results of Ni determination in samples Ni2 – Ni4 by AAS showed an average composition of 64.3 ± 0.2% Ni (calculated for NiS: 64.7% Ni) while for samples Ni5 and Ni6 the results (64.4 ± 0.3%) were even closer to the calculated value.

The UV–Vis spectra of NiS samples, obtained sonochemically by using different amplitudes, are shown in Fig. 4. A baseline correction was applied for all curves. The transmission edges (λ_{max}) were observed at 330, 360 and 375 nm for samples obtained by 50%, 70% and 90% amplitude, respectively. The corresponding optical band gap energies were calculated from Tauc plots using the equation:

http://dx.doi.org/10.1016/j.heliyon.2017.e00273

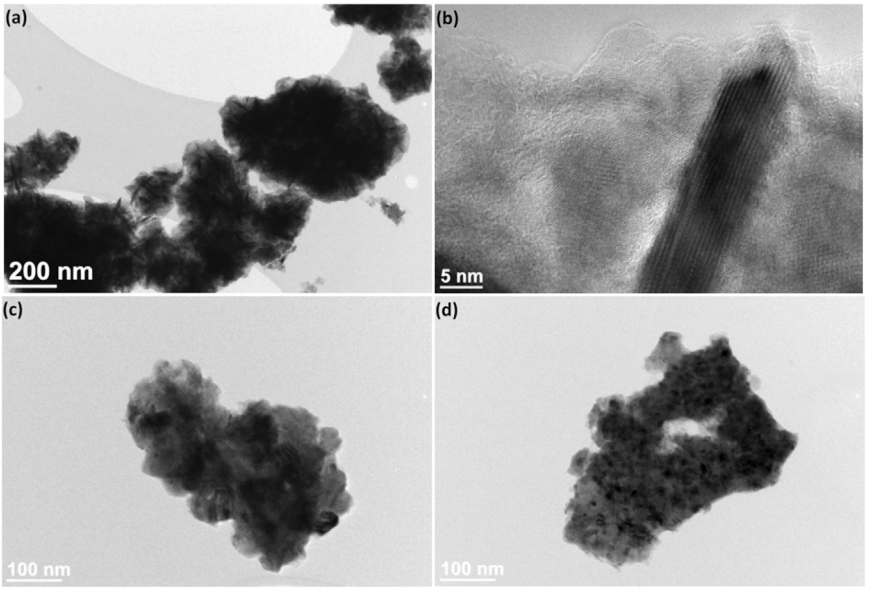

Fig. 3. TEM images of NiS synthesized from $Ni(CH_3COO)_2 \cdot 4H_2O$ and C_2H_5NS (molar ratio 1:1, 1 h sonication time) by using different amplitudes: 50% (a, b), 70% (c) and 90% (d).

$$(\alpha h\nu)^n = A(h\nu - E_g)$$

A plot between $(\alpha h\nu)^2$ vs. $(h\nu)$ was drawn, α being the absorption coefficient and $h\nu$ the photon energy, while $n = 2$ for a direct transition. By extrapolating the linear portion of the curve to the *x*-axis, one can obtain E_g as the intercept [14, 61]. The corresponding E_g values for NiS samples obtained by 50%, 70% and 90% amplitude were 3.8 eV, 3.5 eV and 3.3 eV. It is obvious from the results that the absorption decreases with increasing crystallite size, while the optical band gap

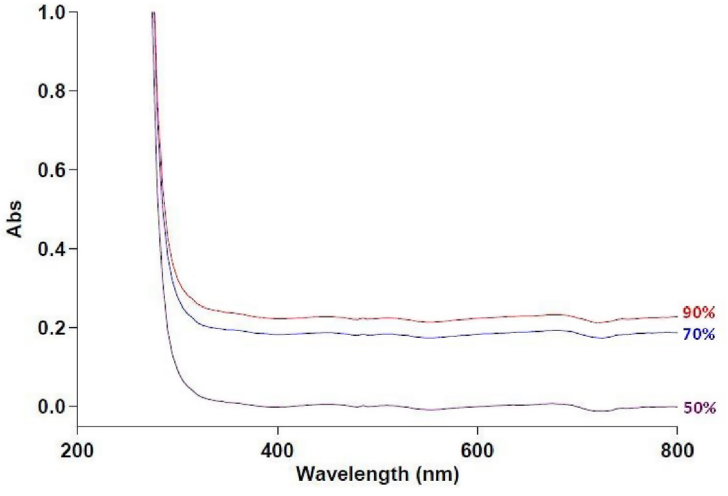

Fig. 4. UV–Vis spectra of NiS samples synthesized from $Ni(CH_3COO)_2 \cdot 4H_2O$ and C_2H_5NS (molar ratio 1:1, 1 h sonication time) by using different amplitudes.

http://dx.doi.org/10.1016/j.heliyon.2017.e00273

energy is higher for lower grain size particles. The calculated optical band gap energy shows a significant blue shift over that of bulk NiS (~ 2.1 eV) [61] which is in close agreement with those published recently for nanosized NiS [14, 62].

Fig. 5a presents the FT-IR spectrum for the prepared NiS nanoparticles. Broad bands between 3400 and 3100 cm^{-1} can be attributed to water adsorbed to the surface of the sample while bands at 394, 419, 442, 668 and 765 (symmetrical stretch) and 1060 cm^{-1} (asymmetrical stretch) are assigned to sulfides, which is in fair agreement to results published for nanosized NiS [14, 63].

Experiments performed with sulfur sources other than thioacetamide were less successful. In cases where thiourea was used as sulfur precursor, only $Ni(OH)_2$ was detected after the reaction. Preliminary results of experiments where $Na_2S_2O_3 \cdot 5H_2O$ and a molar ratio n(Ni):n(S) = 1:1 was used, show the presence of a low-crystallinity product containing NiS and Ni_3S_4 in low yield (sample Ni10). By changing the n(Ni): n(S) ratio to 1:2, nanosized cubic Ni_3S_4 (PDF No. 00-047-1739) with traces of rhomboedral β-NiS (PDF No. 00-003-0760) was obtained, as shown in Fig. 6 (sample Ni11). The AAS analysis showed that the sample Ni11 contained 58.6% Ni, which is higher than the calculated value for Ni_3S_4 (57.9%), confirming the results of XRD measurements.

3.2. Cobalt sulfides

The black powders obtained after the sonochemical syntheses from $Co(CH_3COO)_2 \cdot 2H_2O$ and thioacetamide in different molar ratios were in all cases amorphous. To obtain crystalline products, subsequent heating was necessary. Heating at 400 °C still produced amorphous products, while nanocrystalline products were obtained by heating the precursors obtained by the sonochemical reaction for 2 h at 500 °C.

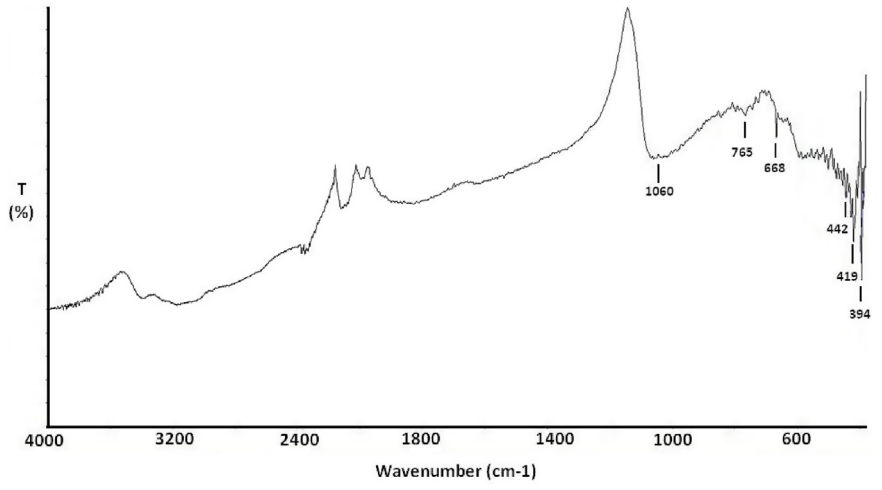

Fig. 5. FT-IR spectrum of NiS nanoparticles prepared via the sonochemical method.

http://dx.doi.org/10.1016/j.heliyon.2017.e00273

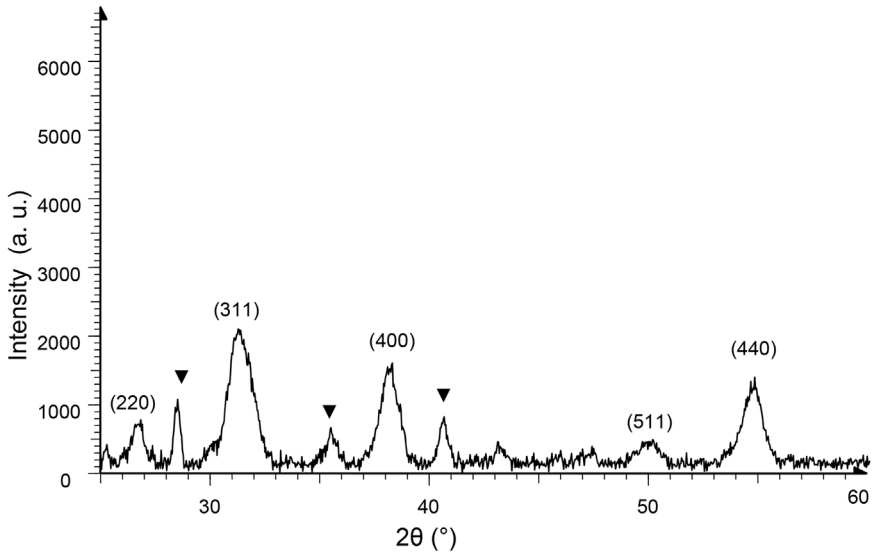

Fig. 6. X-ray powder diffraction pattern of nickel sulfides synthesized from $Ni(CH_3COO)_2 \cdot 4H_2O$ and $Na_2S_2O_3 \cdot 5H_2O$ (molar ratio 1:2, 1 h sonication time). The indexed peaks can be assigned to Ni_3S_4. ▼ = β-NiS.

The TGA results show that the mass of the powder decreased by approximately 7% during heating. Fig. 7 represents the XRD patterns of the products synthesized using various n(Co): n(S) molar ratios. Hexagonal $CoS_{1.097}$ (PDF No. 00-019-0366) was prepared from an equimolar mixture as well as from mixtures where a molar ratio n (Co): n(S) = 1: 2 was used. On the contrary, cubic Co_9S_8 (PDF No. 00-019-0364) was

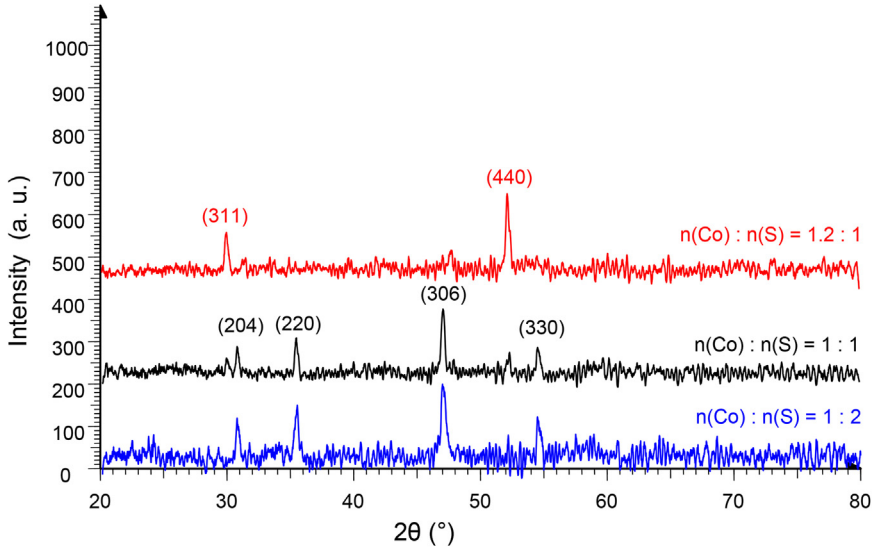

Fig. 7. X-ray powder diffraction pattern of cobalt sulfides synthesized from $Co(CH_3COO)_2 \cdot 2H_2O$ and $Na_2S_2O_3 \cdot 5H_2O$ by using different molar ratio of precursors. The indexed peaks on both lower patterns can be assigned to $CoS_{1.097}$ while both prominent peaks on the upper pattern belong to Co_9S_8.

http://dx.doi.org/10.1016/j.heliyon.2017.e00273

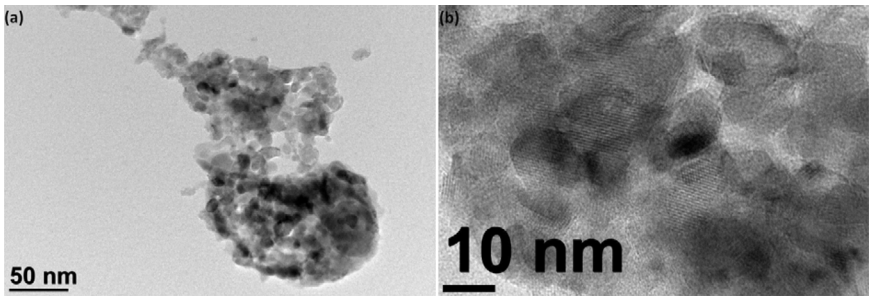

Fig. 8. TEM images of Co_9S_8 nanoparticles synthesized from $Co(CH_3COO)_2 \cdot 2H_2O$ and $Na_2S_2O_3 \cdot 5H_2O$ (molar ratio 1.2:1, 1 h sonication time).

obtained when a 20% excess of cobalt was used during the synthesis. The results indicate that the composition of the products can be simply changed by using different molar ratio of precursors during sonication. Attempts to prepare cobalt sulfides using either thiourea or $Na_2S_2O_3 \cdot 5H_2O$ instead of TAA were unsuccessful, yielding only CoO in both cases.

TEM images of sonochemically prepared Co_9S_8 (Fig. 8a, b) reveal polygonal nanoparticles with average diameters of 20–30 nm, agglomerated into porous clusters. By the EDX analysis we were only able to estimate the atomic ratio Co:S close to 1:1, while the results of the Co analysis by AAS confirmed the observations by XRD: measured 67.3% Co, calculated 67.4% Co. The optical band gap energy for Co_9S_8 nanoparticles was calculated from UV–Vis spectra as described above. The results ($\lambda_{max} = 365$ nm; $E_g = 3.4$ eV) are slightly higher than those reported in recent literature [64], which can be attributed to strong dependence of the optical band gap on the crystallite size. The FT-IR spectrum of

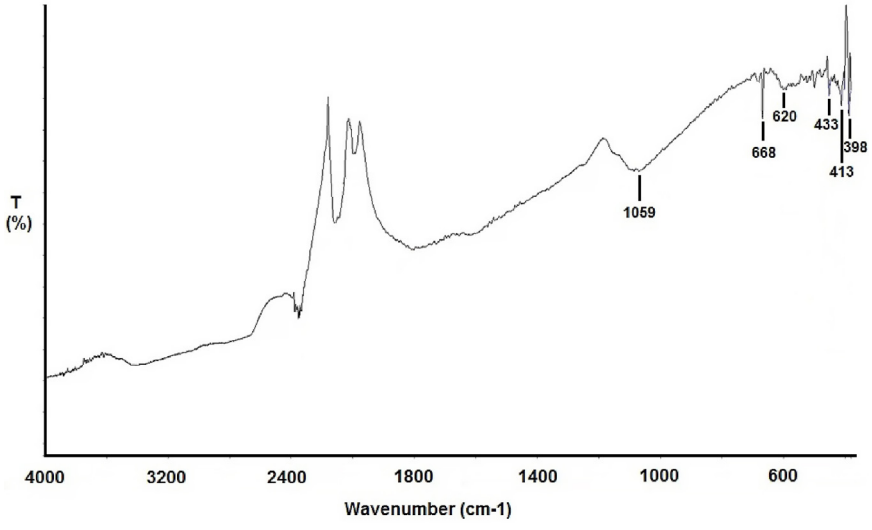

Fig. 9. FT-IR spectrum of Co_9S_8 nanoparticles prepared via the sonochemical method.

http://dx.doi.org/10.1016/j.heliyon.2017.e00273

sonochemically prepared Co_9S_8 (Fig. 9) resembles that of NiS with sulfide stretching bands at 398, 413, 433, 668, and 1059 cm^{-1}. The small peak at 620 cm^{-1} should correspond to stretching vibrations of Co atoms on the surface of Co_9S_8 [64]. A summary of the syntheses performed within this study as well as the obtained products is given in Table 1.

4. Conclusion

Nickel and cobalt sulfides with different stoichiometries, namely, NiS, Ni_3S_4, $CoS_{1.097}$ and Co_9S_8, have been synthesized by the sonochemical method. Various experimental parameters like sulfur precursors, molar ratio of the precursors, the role of complexing agents, sonication time and power were investigated. NiS synthesized from Ni acetate and thioacetamide was studied in detail, showing how the morphology of the product and the optical band gap energy can be altered by increasing the power of ultrasonic irradiation. The ultrasonic method has shown advantages when compared to other methods which are nowadays used for the preparation of sulfide nanoparticles: short reaction times, good yields, easy control of the process. All of the syntheses were performed in aqueous solutions, avoiding the use of organic solvents and toxic precursors, thus contributing to green chemistry approaches.

Declarations

Author contribution statement

Matjaž Kristl: Conceived and designed the experiments; Performed the experiments; Contributed reagents, materials, analysis tools or data; Wrote the paper.

Brina Dojer, Janja Kristl: Performed the experiments.

Sašo Gyergyek: Analyzed and interpreted the data.

Funding statement

This research did not receive any specific grant from funding agencies in the public, commercial, or not-for-profit sectors.

Competing interest statement

The authors declare no conflict of interest.

Additional information

No additional information is available for this paper.

http://dx.doi.org/10.1016/j.heliyon.2017.e00273

Acknowledgements

The authors wish to thank Mr. Jernej Simonič for his help with the laboratory work and Professor Emeritus Miha Drofenik for valuable discussions. The authors also acknowledge the use of equipment in the Center of Excellence on Nanoscience and Nanotechnology – Nanocenter.

References

[1] M.-R. Gao, Y.-F. Xu, J. Jiang, S.-H. Yu, Nanostructured metal chalcogenides: synthesis, modification, and applications in energy conversion and storage devices, Chem. Soc. Rev. 42 (2013) 2986–3017.

[2] S.V. Kershaw, A.S. Susha, A.L. Rogach, Narrow bandgap colloidal metal chalcogenide quantum dots: synthetic methods, heterostructures, assemblies, electronic and infrared optical properties, Chem. Soc. Rev. 42 (2013) 3033–3087.

[3] G.Z. Wang, W. Chen, C.H. Liang, Y.W. Wang, G.W. Meng, L.D. Zhang, Preparation and characterization of CdS nanoparticles by ultrasonic irradiation, Inorg. Chem. Commun. 4 (2001) 208–210.

[4] M. Behboudnia, B. Khanbabaee, Conformational study of CdS nanoparticles prepared by ultrasonic waves, Colloids Surf. A 290 (2006) 229–232.

[5] M. Kristl, I. Ban, A. Danč, V. Danč, M. Drofenik, A sonochemical method for the preparation of cadmium sulfide and cadmium selenide nanoparticles in aqueous solutions, Ultrason. Sonochem. 17 (2010) 916–922.

[6] M. Behboudnia, M.H. Majlesara, B. Khanbabaee, Preparation of ZnS nanorods by ultrasonic waves, Mater. Sci. Eng. B 122 (2005) 160–163.

[7] R.V. Kumar, O. Palchik, Y. Koltypin, Yu. Diamant, A. Gedanken, Sonochemical synthesis and characterization of Ag_2S/PVA and CuS/PVA nanocomposite, Ultrason. Sonochem. 9 (2002) 65–70.

[8] M. Kristl, S. Gyergyek, J. Kristl, Synthesis and characterization of nanosized silver chalcogenides under ultrasonic irradiation, Mater. Express 5 (2015) 359–366.

[9] J.-Z. Xu, S. Xu, J. Geng, G.-X. Li, J.-J. Zhu, The fabrication of hollow spherical copper sulfide nanoparticles assemblies with 2-hydroxypropyl-β-cyclodextrin as a template under sonication, Ultrason. Sonochem. 13 (2006) 451–454.

[10] H. Xu, W. Wang, W. Zhu, Sonochemical synthesis of crystalline CuS nanoplates via an in situ template route, Mater. Lett. 60 (2006) 2203–2206.

 http://dx.doi.org/10.1016/j.heliyon.2017.e00273

[11] M. Kristl, N. Hojnik, S. Gyergyek, M. Drofenik, Sonochemical preparation of copper sulfides with different phases in aqueous solutions, Mater. Res. Bull. 48 (2013) 1184–1188.

[12] D. Mondal, G. Villemure, C. Song, Synthesis, characterization, and evaluation of unsupported porous NiS submicrometer spheres as cathode material for lithium batteries, J. Appl. Electrochem. 44 (2014) 599–606.

[13] P.-F. Yin, L.-L. Sun, C. Zhou, Y.-H. Sun, X.-Y. Han, C.-R. Deng, Characterization and magnetic property of 3D flower-like nickel sulphide nanocrystals through decomposing bis(thiourea) nickel(II) chloride crystals, Bull. Mater. Sci. 38 (2015) 95–99.

[14] S. Surendran, K.V. Sankar, L.J. Berchmans, R.K. Selvan, Polyol synthesis of α-NiS particles and its physic-chemical properties, Mater. Sci. Semicond. Process. 33 (2015) 16–23.

[15] H.-J. Kim, T.-B. Yeo, S.-K. Kim, S.S. Rao, A.D. Savariraj, K. Prabakar, C.V. V.M. Gopi, Optimal-Temperature-Based Highly Efficient NiS Counter Electrode for Quantum-Dot-Sensitized Solar Cells, Eur. J. Inorg. Chem (2014) 4281–4286.

[16] H.-J. Kim, S.-W. Kim, C.V.V.M. Gopi, S.-K. Kim, S.S. Rao, M.-S. Jeong, Improved performance of quantum dot-sensitized solar cells adopting a highly efficient cobalt sulfide/nickel sulfide composite thin film counter electrode, J. Power Sources 268 (2014) 163–170.

[17] C.V.V.M. Gopi, S.S. Rao, S.-K. Kim, D. Punnoose, H.-J. Kim, Highly effective nickel sulfide counter electrode catalyst prepared by optimal hydrothermal treatment for quantum dot-sensitized solar cells, J. Power Sources 275 (2015) 547–556.

[18] C.-C. Sun, M.-Z. Ma, J. Yang, Y.-F. Zhang, P. Chen, W. Huang, X.-C. Dong, Phase-controlled synthesis of alpha-NiS nanoparticles confined in carbon nanorods for high performance supercapacitors, Sci. Rep. 4 (2014) 7054.

[19] H.-C. Chen, J.-J. Jiang, Y.-D. Zhao, L. Zhang, D.-Q. Guo, D.-D. Xia, One-pot synthesis of porous nickel cobalt sulphides: tuning the composition for superior pseudocapacitance, J. Mater. Chem. A 3 (2015) 428–437.

[20] L. Yu, B. Yang, Q. Liu, J. Liu, X. Wang, D. Song, J. Wang, X. Jing, Interconnected NiS nanosheets supported by nickel foam: Soaking fabrication and supercapacitors application, J. Electroanal. Chem. 739 (2015) 156–163.

[21] Y. Wang, Q.-S. Zhu, L. Tao, X.-W. Su, Controlled synthesis of NiS hierarchical hollow microspheres with different building blocks and their application in lithium batteries, J. Mater. Chem. 21 (2011) 9248–9254.

 http://dx.doi.org/10.1016/j.heliyon.2017.e00273

[22] H.-C. Tao, X.-L. Yang, L.-L. Zhang, B.-B. Ni, One step synthesis of nickel sulfide/N-doped graphene composite as anode material for lithium ion batteries, J. Electroanal. Chem. 739 (2015) 36–42.

[23] Z.-J. Zhang, H.-L. Zhao, Z.-P. Zeng, C.-H. Gao, J. Wang, Q. Xia, Hierarchical architecture NiS@SiO_2 nanoparticles enveloped in graphene sheets as anode material for lithium ion batteries, Electrochim. Acta 155 (2014) 85–92.

[24] F.A. Cotton, G. Wilkinson, Advanced Inorganic Chemistry, 4th ed., John Wiley and Sons, New York, 1980.

[25] T. Kosmač, D. Maurice, T.H. Courtney, Synthesis of nickel sulfides by mechanical alloying, J. Am. Ceram. Soc. 76 (1993) 2345–2352.

[26] S. Nagaveena, C.K. Mahadevan, Preparation by a facile method and characterization of amorphous and crystalline nickel sulfide nanophases, J. Alloys Compd. 582 (2014) 447–456.

[27] S. Chen, K. Zeng, H. Li, F. Li, Phase-controlled solvothermal synthesis and characterization of nickel sulfides with good single crystalline nature, J. Solid State Chem. 184 (2011) 1989–1996.

[28] J. Yang, W. Guo, D. Li, C. Wei, H. Fan, L. Wu, W. Zheng, Synthesis and electrochemical performances of novel hierarchical flower-like nickel sulfide with tunable number of composed nanoplates, J. Power Sources 268 (2014) 113–120.

[29] P.-F. Yin, C. Zhou, X.-Y. Han, Z.-R. Zhang, C.H. Xia, L.L. Sun, Shape and phase evolution of nickel sulfide nano/microcrystallines via a facile way, J. Alloys Compd. 620 (2015) 42–47.

[30] M. Salavati-Niasari, G. Banaiean-Monafred, H. Emadi, M. Enhessari, Synthesis and characterization of nickel sulfide nanoparticles via cyclic microwave radiation, C.R. Chim. 16 (2013) 929–936.

[31] V.A.V. Schmachtenberg, G. Tontini, J.A. Koch, G.D.L. Semione, V. Drago, Low temperature solventless syntheses of nanocrystalline nickel sulfides with different sulfur sources, J. Phys. Chem. Solids 87 (2015) 253–258.

[32] F. Luo, J. Li, H. Yuan, D. Xiao, Rapid synthesis of three-dimensional flower-like cobalt sulfide hierarchitectures by microwave assisted heating method for high-performance supercapacitors, Electrochim. Acta 123 (2014) 183–189.

[33] L.P. Mgabi, B.S. Dladla, M.A. Malik, S.S. Garje, J. Akhtar, N. Revaprasadu, Deposition of cobalt and nickel sulfide thin films from thio- and alkylthio-urea

 http://dx.doi.org/10.1016/j.heliyon.2017.e00273

complexes as precursors via the aerosol assisted chemical vapour deposition technique, Thin Solid Films 564 (2014) 51–57.

[34] S.-J. Bao, Y. Li, C.M. Li, Q. Bao, Q. Lu, J. Guo, Shape evolution and magnetic properties of cobalt sulfide, Cryst. Growth Des. 8 (2008) 3745–3749.

[35] R.C. Hoodless, R.B. Moyes, P.B. Wells, D-tracer study of butadiene hydrogenation and tertahydrothiophen hydrodesulphurization catalysed by Co_9S_8, Catal. Today 114 (2006) 377–382.

[36] S.A. Patil, D.V. Shinde, I. Lim, K. Cho, S.S. Bhande, R.S. Mane, N.K. Shresta, J.K. Lee, T.H. Yoon, S.-H. Han, An ion exchange mediated shape-perserving strategy for constructing 1-D arrays of porous $CoS_{1.0365}$ nanorods for electrocatalytic reduction of triiodide, J. Mater. Chem. A 3 (2015) 7900–7909.

[37] L.-L. Feng, G.-D. Li, Y.-P. Liu, Y.-Y. Wu, H. Chen, Y. Wang, Y.-C. Zou, D.-J. Wang, X.-X. Zou, Carbon-armored Co_9S_8 nanoparticles as all-pH efficient and durable H_2-evolving electrocatalysts, ACS Appl. Mater. Interfaces 7 (2015) 980–988.

[38] N. Rumale, S. Arbuj, G. Umarji, M. Shinde, U. Mulik, P. Joy, D. Amalnerkar, Tuning Magnetic Behavior of Nanoscale Cobalt Sulfide and its Nanocomposite with an Engineering Thermoplastic, J. Electron. Mater. 44 (2015) 2308–2311.

[39] L.-J. Sun, Y. Bai, K.-N. Sun, Organic molecule controlled synthesis of three-dimensional rhododendron-like cobalt sulfide hierarchitectures as counter electrodes for dye-sensitized solar cells, RSC Adv. 4 (2014) 42087–42091.

[40] M. Congiu, L.G.S. Albano, F. Decker, C.F.O. Graeff, Single precursor route to efficient sulphide counter electrodes for dye sensitized solar cells, Electrochim. Acta 151 (2015) 517–524.

[41] Y.-D. Luo, J. Shen, R. Cheng, X.-H. Chen, Y.-W. Chen, Z. Sun, S.-M. Huang, Facile synthesis of mixed-phase cobalt sulfide counter electrodes for efficient dye sensitized solar cells, J. Mater. Sci.: Mater. Electron. 26 (2015) 42–48.

[42] Z.-P. Li, W.-Y. Li, H.-T. Xue, W.-P. Kang, X. Yang, M.-L. Sun, Y.-B. Tang, C.-S. Lee, Facile fabrication and electrochemical properties of high-quality reduced graphene oxide/cobalt sulfide composite as anode material for lithium-ion batteries, RSC Adv. 4 (2014) 37180–37186.

[43] Y.-L. Zhou, D. Yan, H.-Y. Xu, J.-K. Feng, X.-L. Jiang, J. Yue, J. Yang, Y.-T. Qian, Hollow nanospheres of mesoporous Co_9S_8 as a high-capacity and

long-life anode for advanced lithium ion batteries, Nano Energy 12 (2015) 528–537.

[44] Q. Wang, R. Zou, W. Xia, J. Ma, B. Qiu, A. Mahmood, R. Zhao, Y. Yang, D. Xia, Q. Xu, Facile synthesis of ultrasmall CoS_2 nanoparticles within thin N-doped porous carbon shell for high performance lithium-ion batteries, Small 11 (2015) 2511–2517.

[45] Q. Chen, H. Li, C. Cai, S. Yang, K. Huang, X. Weiab, J. Zhong, In situ shape and phase transformation synthesis of Co_3S_4 nanosheet arrays for high-performance electrochemical supercapacitors, RSC Adv. 3 (2013) 22922-–22926.

[46] H. Wan, X. Ji, J. Jiang, J. Yu, L. Miao, L. Zhang, S. Bie, H. Chen, Y. Ruan, Hydrothermal synthesis of cobalt sulfide nanotubes: The size control and its application in supercapacitors, J. Power Sources 243 (2013) 396–402.

[47] K.-J. Huang, J.-Z. Zhang, G.-W. Shi, Y.-M. Liu, One-step hydrothermal synthesis of two-dimensional cobalt sulfide for high-performance super-capacitors, Mater. Lett. 131 (2014) 45–48.

[48] B. You, N. Jiang, M. Sheng, Y. Sun, Microwave vs. solvothermal synthesis of hollow cobalt sulfide nanoprisms for electrocatalytic hydrogen evolution and supercapacitors, Chem. Commun. 51 (2015) 4252–4255.

[49] H. Emadi, M. Salavati-Niasari, F. Davar, Synthesis and characterization of cobalt sulfide nanocrystals in the presence of thioglycolic acid via a simple hydrothermal method, Polyhedron 31 (2012) 438–442.

[50] N. Kumar, N. Raman, A. Sundaresan, Z. Anorg, Synthesis and properties of cobalt sulfide phases: CoS_2 and Co_9S_8, Allg. Chem. 640 (2014) 1069–1074.

[51] T. Rajabloo, A. Ghafarinazari, L.S. Faraji, M. Mozafari, Taguchi based fuzzy logic optimization of multiple quality characteristics of cobalt disulfide nanostructures, J. Alloys Compd. 607 (2014) 61–66.

[52] M. Salavati-Niasari, M. Sabet, E. Esmaeili, Synthesis and characterization of CoS_2 nanostrucures via hydrothermal method, Synth. React. Inorg., Met.-Org Nano-Met. Chem. 45 (2015) 1159–1167.

[53] M.M. Mdleleni, T. Hyeon, K.S. Suslick, Sonochemical synthesis of nanostructured molybdenum sulfide, J. Am. Chem. Soc. 120 (1998) 6189–6190.

[54] K.S. Suslick, Sonochemistry, Science 247 (1990) 1439–1445.

[55] A. Gedanken, Using Sonochemistry for the fabrication of nanomaterials, Ultrason. Sonochem. 11 (2004) 47–55.

 http://dx.doi.org/10.1016/j.heliyon.2017.e00273

[56] J.H. Bang, K.S. Suslick, Applications of ultrasound to the synthesis of nanostructured materials, Adv. Mater. 22 (2010) 1039–1059.

[57] M. Kristl, J. Kristl, Sonochemical process for the preparation of nanosized copper selenides with different phases, Chalcogenide Lett. 11 (2014) 59–66.

[58] H. Wang, J.-R. Zhang, X.-N. Zhao, S. Xu, J.-J. Zhu, Preparation of copper monosulfide and nickel monosulfide nanoparticles by sonochemical method, Mater. Lett. 55 (2002) 253–258.

[59] S.M. de la Parra-Arciniega, N.A. García-Gómez, D.I. Garcia-Gutierrez, P. Salinas-Estevané, E.M. Sánchez, Ionic liquid assisted sonochemical synthesis of NiS submicron particles, Mater. Sci. Semicond. Process. 23 (2014) 7–13.

[60] A. Askarinejad, A. Morsali, Direct ultrasonic-assisted synthesis of sphere-like nanocrystals of spinel Co_3O_4 and Mn_3O_4, Ultrason. Sonochem. 16 (2009) 124–131.

[61] S. Jana, S. Samai, B.C. Mitra, P. Bera, A. Mondal, Nickel oxide thin film from electrodeposited nickes sulfide thin film: peroxide sensing and photo-decomposition of phenol, Dalton Trans. 43 (2014) 13096–13104.

[62] X. Shen, J. Sun, G. Wang, J. Park, K. Chen, A facile single-source approach to urchin-like NiS nanostructures, Mat. Res. Bull. 45 (2010) 766–771.

[63] Y. Fazli, S.M. Pourmortazavi, I. Kohsari, M. Sadeghpur, Electrochemical synthesis and structure characterization of nickel sulfide nanoparticles, Mater. Sci. Semicond. Process. 27 (2014) 362–367.

[64] R. Ramachandran, M. Saranya, C. Santosh, V. Velmurguran, B.P.C. Raghupathy, S.K. Jeong, A.N. Grace, Co_9S_8 nanoflakes on graphene (Co_9S_8/G) nonocomposites for high performance supercapacitors, RSC Adv. 4 (2014) 21151–21162.

 http://dx.doi.org/10.1016/j.heliyon.2017.e00273